# Link Energy Minimization in IR-UWB Based Wireless Networks

Tianqi Wang, *Student Member, IEEE,* Wendi Heinzelman, *Senior Member, IEEE,* and Alireza Seyedi, *Member, IEEE*

***Abstract*—Impulse Radio Ultra WideBand (IR-UWB) communication has proven to be an important technique for supporting high-rate, short-range, and low-power communication. In this paper, using detailed models of typical IR-UWB transmitter and receiver structures, we model the energy consumption per information bit in a single link of an IR-UWB system, considering packet overhead, retransmissions, and a Nakagami-m fading channel. Using this model, we minimize the energy consumption per information bit by finding the optimum packet length and the optimum number of RAKE fingers at the receiver for different transmission distances, using Differential Phase-shift keying (DBPSK), Differential Pulse-position Modulation (DPPM) and On-off Keying (OOK), with coherent and non-coherent detection. Symbol repetition schemes with hard decision (HD) combining and soft decision (SD) combining are also compared in this paper. Our results show that at very short distances, it is optimum to use large packets, OOK with non-coherent detection, and HD combining, while at longer distances, it is optimum to use small packets, DBPSK with coherent detection, and SD combining. The optimum number of RAKE fingers are also found for given transmission schemes.**

***Index Terms*—Impulse radio ultra wideband, link energy minimization, energy consumption, packetization, ARQ, RAKE receiver.**

## I. Introduction

IMPULSE radio ultra wideband (IR-UWB) communications is regarded as an attractive solution to provide high bandwidth and low radiated power, especially for short-range wireless network applications [1]-[4]. Wireless sensor networks (WSNs) have been used for applications ranging from environmental monitoring and health monitoring to security and surveillance [5][6]. These different applications for WSNs have vastly different bandwidth requirements. Take, for example, visual sensor networks (VSNs) for surveillance or health monitoring. These networks require a relatively large bandwidth to transmit and receive images or video in a timely manner, and a low radiated power to avoid interference with coexisting wireless systems. IR-UWB technology, in this case, has a great potential to facilitate the application of VSNs.

Manuscript received July 14, 2009; revised December 19, 2009 and May 2, 2010; accepted June 29, 2010. The associate editor coordinating the review of this paper and approving it for publication was P. Popovski.

The authors are with the Department of Electrical and Computer Engineering, University of Rochester, USA (e-mail: {tiwang, wheinzel, alireza}@ece.rochester.edu).

This work was supported in part by the National Science Foundation under grant # ECS-0428157 and in part by a Young Investigator grant from the Office of Naval Research, # N00014-05-1-0626.

Digital Object Identifier 10.1109/TWC.2010.072110.091038

Energy consumption is a very important design consideration in any IR-UWB based system. Unlike in traditional communications systems, where transmit power can be flexibly adjusted to minimize the energy consumption [7][8], there is a strict limit on the effective isotropic radiated power (EIRP) in IR-UWB systems due to their overlay nature. Regulations mandate that the spectrum of the signal be limited to $-41.25$ dBm/MHz [1]. Since the IR-UWB system needs to operate at or near this limit to achieve a reasonable range, the traditional optimization techniques, which mainly operate by adjusting the transmit power, cannot be used for IR-UWB systems. However, there are other parameters of the IR-UWB system that can be adjusted, such as the number of RAKE fingers, the packet length, the modulation scheme, the detection scheme, and the coding or spreading scheme.

In IR-UWB communications, the channel delays are often resolvable due to the narrow width of the IR-UWB pulse. Therefore, a RAKE receiver structure can achieve considerable diversity gain [9][10]. Another important utility of the RAKE receiver structure is that it can increase the collection of the transmitted power through multiple paths. The diversity gain and collected power will be increased by adding more RAKE fingers (correlator taps), which in turn will increase the power consumption of the receiver. Therefore, the tradeoff between the diversity gain as well as the power collection and the power consumption at the receiver must be evaluated.

Packet length is another important factor that influences the energy consumption of a communication link. A long packet will increase the packet error probability; thereby increasing the average number of transmissions in an automatic-repeat-request (ARQ) system. On the other hand, a short packet will lower the system efficiency due to the packet overhead. Thus, an optimum packet length should be found to minimize the energy consumption.

Binary modulation schemes, such as DBPSK, OOK, and DPPM, are usually used in IR-UWB systems due to their simplicity and good performance. Among the three modulation schemes considered in this paper (DBPSK, OOK, and DPPM), DBPSK is the most robust, but also the most energy consuming. Compared with DBPSK, OOK requires less energy to transmit each bit, but has a lower performance. The performance of DPPM is between DBPSK and OOK. The comparison and evaluation of these modulation schemes are important for the design of energy-efficient IR-UWB systems.

In our previous work, we proposed an energy consumption model of an IR-UWB based communication link, and we

compared the energy consumption features of DBPSK/OOK modulations with coherent/noncoherent detections schemes [11]. Compared with the preliminary work in [11], here we comprehensively analyze the theoretic energy consumption characteristics of an IR-UWB communication link and provide an extensive comparison of practical schemes. Moreover, we use a more realistic Nakagami-m fading channel model to describe the wireless channel in an IR-UWB system.

In this paper, we provide detailed power consumption models of a typical IR-UWB transmitter and both coherent and noncoherent receivers. The optimization model considers these detailed power consumption models as well as the packet structure and the ARQ procedure. Using this model we optimize packet length and the number of RAKE fingers at different transmission distances for DBPSK, OOK, and DPPM, with both coherent (CO) and noncoherent (NC) detection. Moreover, in IR-UWB systems, to increase the effective energy per bit, repetition coding schemes are commonly used. At the receiver, hard decision (HD) based combining or soft decision (SD) based combining may be used. HD combining provides relatively low performance but it can be operated using a low-power, one bit analog-to-digital converter (ADC). On the other hand, SD combining provides good performance while demanding a high-resolution ADC and memory units. The tradeoffs between these combining methods are also evaluated in this paper.

The remainder of this paper is organized as follows. Section II surveys related work. Section III introduces the packet structure, transceiver power model, and channel model used in this paper. In Section IV, after deriving a lower bound on the energy consumption per information bit in IR-UWB systems, we minimize the energy consumption per information bit over packet length and number of RAKE fingers. Numerical results are presented in Section V. Section VI concludes this paper.

## II. Related Work

Some related work has been conducted on the improvement of link energy efficiency for battery-powered networks. Cui *et al.* studied the energy per information bit minimization problem for narrowband systems, considering the dependency of circuit power consumption due to modulation and coding schemes and the time duration of a packet containing $L$ information bits for different coding schemes [8]. The authors proposed detailed power models of a typical narrowband transmitter and receiver and clearly pointed out the dependency of the power consumption on physical layer configurations, such as modulation schemes and coding schemes. They also extended their work to energy minimization in cooperative MIMO based networks, considering increased spectral efficiency and circuit power consumptions [12]. However, the effects of an ARQ scheme or the optimum selection of target bit error probability were not considered.

In [13], Ammer and Rabaey proposed the energy-per-useful-bit (EPUB) metric to measure the PHY efficiency of wireless networks. The authors conclude that to minimize EPUB, high data rates, low carrier frequencies, and simple modulation schemes are preferred. The authors also point out that the packet header plays an important role in evaluating EPUB and should be fully studied. The authors limited their research to low order modulations and assumed variable signal bandwidth, which may constrain the application of their results.

Lu *et al.* find an optimal configuration of source encoder, channel encoder and transmitter for a fixed end-to-end source distortion to minimize the power consumption of a multimedia communication link over an AWGN channel [14]. The optimization parameters in [14] are source coding rates and channel coding rates.

Besides modulation schemes, coding rates and carrier frequencies, the impact of packet size on the performance of wireless networks has also been investigated and proven to be significant [15][16]. The investigation of energy minimization over a frequency-selective channel that requires a more complicated receiver structure, such as a RAKE receiver, has not been studied in the literature. In this paper, we focus on IR-UWB systems and jointly consider the effects of the repetition coding, the modulation scheme, the detection scheme, the combining scheme, the packet length, and the number of RAKE fingers.

Among the numerous enabling communication technologies for wireless networks, IR-UWB is intriguing due to its low-power high-rate feature. The performance of IR-UWB has been extensively studied [17]-[19]. Some work on the optimization of IR-UWB systems considering antenna design, synchronization and channel capacity are also present in the literature [20]-[23]. However, none of these optimizations is aimed at minimizing the energy consumption in IR-UWB systems. The energy capture effect of a RAKE receiver in IR-UWB systems was first studied by Win *et al.* in [24]. The authors analyze the relationship between the diversity level and captured energy. Although no power model is assumed in [24], the authors have concluded that there exists a threshold number of RAKE fingers in IR-UWB systems such that adding more RAKE fingers does not significantly improve performance. Despite the fact that much research has been conducted on IR-UWB systems, a detailed study on link energy minimization in IR-UWB based networks is lacking.

An effective channel model is critical in evaluating the performance of any communication system. Numerous research efforts have been made towards establishing an effective IR-UWB channel model [25]-[27]. In particular, Molisch *et al.* proposed comprehensive IR-UWB channel models for both frequency ranges from $3-10$ GHz and below 1 GHz in 2006 [26]. A single-slope power decay law is adopted to describe the path loss feature of the IR-UWB channel, and Nakagami-distributed amplitude is used to describe the small-scale fading of the IR-UWB channel [26]. This model has been accepted by the IEEE 802.15.4a Task Group as a standard model to evalute UWB systems, and is also used in this paper to evaluate the energy consumption of different schemes.

## III. System and Channel Models

We consider an IR-UWB system with a symbol repetition scheme. The coding rate $R_c = 1/N_p$, where $N_p$, which is an odd number, is the coding parameter. Moreover, in order to avoid inter symbol interference (ISI), the maximum pulse rate is limited. Also, perfect knowledge of the channel is assumed at the receiver.

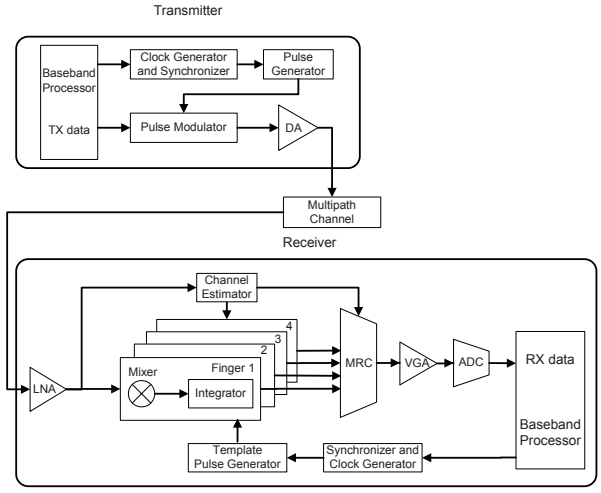


Fig. 1. The transmitter and receiver structure in an IR-UWB system.

### A. IR-UWB Transceiver Power Consumption Model

A typical IR-UWB transmitter and a typical IR-UWB receiver with four RAKE fingers and maximal ratio combining (MRC) are shown in Fig. 1. When DBPSK, DPPM, and OOK are used at the transmitter, the power consumption of the transmitter can be modeled as

$$P_t = P_{\text{SYN}} + E_p R_p, \tag{1}$$

where $E_p$ is the fixed energy per pulse and $R_p$ is the pulse rate. The pulse rate $R_p = \rho_t R_b$, where $\rho_t = 1$ for DBPSK and DPPM, $\rho_t = 0.5$ for OOK, and $R_b$ is the bit rate. We have assumed that an information bit may be 0 or 1 with equal probability. Furthermore, $P_{\text{SYN}}$ represents the power consumption of the transmitter components that are independent from the data transmission, namely the clock generator and synchronizer.

In our model, the power consumption of an IR-UWB transmitter, as described by equation (1), is grouped into two parts: the power consumption from the circuit components that are not related to pulse generating ($P_{\text{SYN}}$), and the power consumption from the ones that are related to pulse generating ($E_p R_p$). That is, $E_p R_p$ includes the power consumptions of the pulse generator, pulse modulator and digital amplifier (DA), while $P_{\text{SYN}}$ is simply the power consumption of the clock generator and synchronizer.

As shown in Fig. 1, the power consumption of an IR-UWB receiver can be modeled as

$$\begin{aligned} P_r \quad &= M P_{\text{COR}} + \rho_c P_{\text{ADC}} + P_{\text{LNA}} + P_{\text{VGA}} \\ &\quad + \rho_r (P_{\text{GEN}} + P_{\text{SYN}} + P_{\text{EST}}), \end{aligned} \tag{2}$$

where $P_{\text{COR}}, P_{\text{ADC}}, P_{\text{LNA}}, P_{\text{VGA}}, P_{\text{GEN}}, P_{\text{SYN}}$, and $P_{\text{EST}}$ respectively represent: the power consumptions of one correlator branch (mixer and integrator), the analog-to-digital converter (ADC), the low noise amplifier (LNA), the variable gain amplifier (VGA), the pulse generator, the synchronizer, and the channel estimator. $M$ represents the number of RAKE fingers at the receiver. $\rho_r$ is determined by the receiver structure. That is, $\rho_r = 1$ for coherent demodulation and $\rho_r = 0$ for noncoherent demodulation. This is because for a noncoherent UWB receiver, the pulse generator, clock generator, synchronizer, and channel estimator are not necessary. Moreover, $\rho_c = 1$ for SD combining and $\rho_c = 0$ for HD combining. For SD combining, a 5-bit ADC is assumed [28], while for HD combining, the power consumption of the ADC (one-bit ADC) is assumed to be negligible.

At the receiver, we consider an IR-UWB receiver that is able to choose the coherent or noncoherent demodulation after the signal passed through RAKE fingers and MRC. When the IR-UWB receiver uses the coherent detection, the received signal will pass through a matched filter and a template pulse needs to be generated to configure the matched filter. When the IR-UWB receiver adopts the noncoherent detection, neither a matched filter nor a template pulse is needed. The received signal will be either correlated with the previously received signal, or simply be multiplied by itself (envelop detection). A differential modulation scheme can cooperate with either the coherent detection or noncoherent detection. For example, a DBPSK modulated signal can be noncoherently detected by a correlation with the previously received signal so that only the difference between the two signals will be at output of the ADC, or each DBPSK modulated signal can be coherently detected individually through a matched filter and the difference between two adjacent bits can be measured in the digital domain. In general, the coherent detection provides a better performance than the noncoherent detection in terms of bit error probability. However, the coherent detection requires more circuit components (template pulse generator, synchronizer, and etc.) and thereby consumes more power than the noncoherent detection.

As with the transmitter, we also group the power consumption of an IR-UWB receiver into two parts: the power consumption of the circuit components that are not related to the detection schemes ($M P_{\text{COR}} + \rho_c P_{\text{ADC}} + P_{\text{LNA}} + P_{\text{VGA}}$), and the power consumption of the circuit components that are related to the detection schemes ($\rho_r (P_{\text{GEN}} + P_{\text{SYN}} + P_{\text{EST}})$). That is, $M P_{\text{COR}} + \rho_c P_{\text{ADC}} + P_{\text{LNA}} + P_{\text{VGA}}$ represents the power consumption of $M$ correlator branches, the ADC, the LNA, and the VGA. These components need to be active whether coherent or noncoherent detection is used at the receiver. However, the pulse generator, the synchronizer, and the channel estimator are only active during coherent detection, where a template pulse has to be generated to correlate with the received pulse and the channel information is required. During noncoherent detection, the pulse generator, the synchronizer and the channel estimator are not necessary because no template pulse is needed and the received signal pulse is only correlated with the previously received pulse. The power consumption of the MRC is not considered, since a MRC is simply an adder.

### B. Packet Structure

The packet structure consists of three components: synchronization preamble (SP), PHY-header (PHR), and payload. We assume that there are $L_L$ bits in the payload, $L_{\text{PHR}}$ bits in the PHR, and $L_{\text{SP}}$ symbols in the SP. Correspondingly, the time durations to deliver the payload, the PHR, and the SP are denoted by $T_{\text{onL}}$, $T_{\text{PHR}}$, and $T_{\text{SP}}$, respectively. The energy

consumption to transmit a packet once is the summation of two parts: $E_O$, the energy consumed on delivering the SP and PHR, and $E_L$, the energy consumed on the payload.

We assume that the synchronization preamble has values {-1, 1}. Moreover, the PHR is modulated using DBPSK and always received coherently. This is to ensure that the PHR is transmitted using the modulation and detection schemes with the highest performance, since the PHR carries important information. Also for the sake of simplicity, we assume that the PHR is coded in the same manner as the payload. Therefore, the overhead energy consumption is

$$\begin{aligned} E_O &= E_O^{(\text{TX})} + E_O^{(\text{RX})} \\ &= (L_{\text{SP}} + L_{\text{PHR}}/R_c)E_p + P_{\text{SYN}}T_O + P_rT_O, \end{aligned} \tag{3}$$

where $L_{\text{SP}}$ is the number of SP symbols, $L_{\text{PHR}}$ is the number of PHR bits, and $T_O = T_{\text{SP}} + T_{\text{PHR}} = (L_{\text{SP}} + \frac{L_{\text{PHR}}}{R_c})/R_{\text{base}}$, where $R_{\text{base}}$ is the fixed base data rate. In this paper, a frequency selective slow fading channel is assumed. Therefore, the channel estimation block consumes $P_{\text{EST}}$ amount of power only during the reception of the overhead.

The energy consumption for the payload can be modeled as

$$E_L = E_L^{(\text{TX})} + E_L^{(\text{RX})}, \tag{4}$$

where $E_L^{(\text{TX})}$ and $E_L^{(\text{RX})}$ represent the energy consumption to transmit/receive the payload containing $L_L$ information bits, respectively. For $E_L^{(\text{TX})}$, we have

$$E_L^{(\text{TX})} = \rho_t E_p L_L/R_c + P_{\text{SYN}}T_{\text{onL}}, \tag{5}$$

where $T_{\text{onL}} = L_L/R_bR_c$, is the time duration to transmit the payload containing $L_L$ bits, and $R_c$ is the coding rate.

The energy consumption to receive $L_L$ information bits is given by

$$\begin{aligned} E_L^{(\text{RX})} &= \rho_t(MP_{\text{COR}} + \rho_c P_{\text{ADC}} + P_{\text{LNA}} + P_{\text{VGA}})T_{\text{onL}} \\ &\quad +\rho_r(P_{\text{GEN}} + P_{\text{SYN}})T_{\text{onL}}. \end{aligned} \tag{6}$$

The receiver does not consume power on channel estimation during the reception of information bits when using either coherent or noncoherent detection, since the channel information has been estimated during the reception of the overhead bits.

### C. Channel Model

The channel model consists of a path loss model and a frequency selective fading model. In this paper, we focus our research on the frequency range from 3-10 GHz.

*1) Path Loss Model:* The UWB path loss model is both distance and frequency dependent and can be modeled as [26]

$$G_d = G_0 - 20(\kappa+1)\log_{10}(\frac{f}{f_c}) - 10n\log_{10} d - 3, \tag{7}$$

where $d$ is the transmission distance, $G_0$ is the path gain at the reference distance ($d = 1$ m), $n$ is the path loss exponent, $f$ is the UWB transmission center frequency, $f_c$ is the reference frequency, and $\kappa$ is the frequency dependency decaying factor. Both $G_d$ and $G_0$ are expressed in dB.

*2) Frequency Selective Fading:* In an IR-UWB system, the transmitted signal inevitably encounters frequency selective fading. The baseband channel impulse response of a frequency selective fading channel in UWB systems consists of clusters and rays and can be represented as [26]

$$c(t) = \sum_{l=0}^{L}\sum_{k=0}^{K} \alpha_{k,l}e^{-\theta_{k,l}}\delta[t - T_l - \tau_{k,l}], \tag{8}$$

where $\theta_{k,l}$ follows a uniform distribution (over $[0, 2\pi]$) and $\alpha_{k,l}$ is the amplitude gain of the *k*th ray in the *l*th cluster. $L$ and $K$ represent the number of clusters and rays, respectively. $T_l$ is the arrival time of the *l*th cluster, and $\tau_{k,l}$ is the arrival time of the *k*th ray in the *l*th cluster. $T_l$ and $\tau_{k,l}$ follow the following independent interarrival exponential probability density functions, the details of which can be found in [26].

The average power gain of the *k*th ray in the *l*th cluster is modeled as

$$\mathbf{E}[\alpha_{k,l}^2] = \mathbf{E}[\alpha_{0,0}^2]e^{-T_l/\Gamma}e^{-\tau_{k,l}/\gamma}, \tag{9}$$

where $\Gamma$ and $\gamma$ are power-delay time constraints for the clusters and rays, respectively. $\mathbf{E}[\alpha_{0,0}^2]$ is the average power gain of the first ray of the first cluster, which is expressed as

$$\mathbf{E}[\alpha_{0,0}^2] = \frac{G_d}{\gamma\lambda}. \tag{10}$$

The parameter $\alpha_{k,l}$ follows a Nakagami distribution described as

$$p(\alpha_{k,l}) = \frac{2}{\Gamma(m)}\left(\frac{m}{\mathbf{E}[\alpha_{k,l}^2]}\right)^m \alpha_{k,l}^{2m-1}e^{-\frac{m\alpha_{k,l}^2}{\mathbf{E}[\alpha_{k,l}^2]}}, \tag{11}$$

where $m > 0.5$ is the Nakagami m-factor and $\Gamma(m)$ is the gamma function.

## IV. Link Energy Minimization

### A. Lower Bound on Average Energy Consumption per Information Bit

*1) Lower bound based on channel capacity:* The transmit power is strictly limited in IR-UWB systems to avoid interfering with pre-existing communication systems. In the following analysis, we assume the transmit power is a constant denoted by $P_{\text{tx}}$. Considering the power consumption at the transmitter and receiver and the channel capacity, the lower bound of energy consumption per information bit is modeled as

$$\begin{aligned} E_b &\geq \frac{P_t+P_r}{B\log(1+\frac{\sum_{i=1}^{M}|\alpha_i|^2P_{\text{tx}}}{G_d\sigma^2})}, \\ &= \frac{P_{\text{SYN}}+E_pR_p+MP_{\text{COR}}+P_{\text{CNST}}}{B\log(1+\frac{\sum_{i=1}^{M}|\alpha_i|^2P_{\text{tx}}}{G_d\sigma^2})}, \end{aligned} \tag{12}$$

where $P_{\text{CNST}} = \rho_c P_{\text{ADC}} + P_{\text{LNA}} + P_{\text{VGA}} + \rho_r(P_{\text{GEN}} + P_{\text{SYN}})$ represents the receiver power consumption that is independent of the number of RAKE fingers, and $|\alpha_i|^2$ represents the average power gain of the *i*th selected path. Note that the power consumption of the channel estimator is not considered, since the channel estimator is not involved in the actual data communication. We assume that the positioning of the RAKE fingers is ideal and therefore $|\alpha_i|^2$ are the largest $M$ values of $\mathbf{E}[|\alpha_{k,l}|^2]$ from (9). $M$ is the number of RAKE fingers, and $B$ is the signal bandwidth. Correspondingly, $B\log(1 + \sum_{i=1}^{M}|\alpha_i|^2P_{\text{tx}}/G_d\sigma^2)$ represents the channel capacity [29].

Equation (12) can be minimized through proper selection of the number of RAKE fingers, $M$. As transmission distance increases, the optimum number of RAKE fingers increases and eventually converges to a certain value. In other words, when received SNR approaches zero, there exists an optimum number of RAKE fingers that minimizes the energy consumption in IR-UWB systems. This optimum number is only a function of the power delay profile of the channel and the power consumption values of the components of the transceiver.

Removing the integer constraint on $M$, we can determine this convergence by finding the discrete derivative of the right hand side of (12) with respect to $M$ and setting the resulting equation to zero, i.e.,

$$\begin{aligned}(\log_2 e)\frac{\sum_{i=1}^{M^*}|\alpha_i|^2}{|\alpha_{M^*}|^2}(1+\frac{\sum_{i=1}^{M^*}|\alpha_i|^2 P_{\text{tx}}}{G_d\sigma^2}) \\ = \frac{P_{\text{CNST}}+P_{\text{SYN}}+R_p\rho_t E_p}{P_{\text{COR}}}+M^*,\end{aligned} \tag{13}$$

where $e$ is the natural number. As distance increases, $M^*$ will eventually converge to a particular value as $\sum_{i=1}^{M^*}|\alpha_i|^2 P_{\text{tx}}/G_d\sigma^2 \to 0$. The convergence value of $M^*$ , which is denoted by $M^*_{\text{CONV}}$, can be found from:

$$(\log_2 e)\frac{\sum_{i=1}^{M^*_{\text{CONV}}}|\alpha_i|^2}{|\alpha_{M^*_{\text{CONV}}}|^2}-\frac{P_{\text{CNST}}+P_{\text{SYN}}+R_p\rho_t E_p}{P_{\text{COR}}} = M^*_{\text{CONV}}. \tag{14}$$

In general, there is no closed form solution for (14), since the distribution of $|\alpha_i|^2$ directly determines the solvability of this equation and $M$ has to be chosen in the positive discrete domain. For the doubly exponential decay of $\mathbf{E}[|\alpha_{k,l}|^2]$, $M^*_{\text{CONV}}$ exists and can always be easily found through an exhaustive search.

*2) Lower bound based on data rate:* During the modeling in (12), the data rate is bounded by the channel capacity, which implies a linear channel (such as an AWGN channel), infinitely long codewords, and arbitrarily low bit error rates (i.e., no retransmissions). Most of the above assumptions do not hold in practical communication systems. Thus, the practical data rate is usually much lower than the channel capacity. The lower bound from (12) is, therefore, a very loose lower bound. In the following analysis, instead of using channel capacity, we derive the lower bound energy consumption per information bit by using achievable data rates. In particular, the data rate needs to consider the penalty caused by retransmission and packetization.

In this paper, we only consider binary modulation schemes. Also, to avoid ISI, the maximum pulse rate is limited by the maximum excess delay of the multipath channel, $D_s$. That is, the maximum pulse rate is $1/D_s$. In addition, considering the impacts of packetization, retransmission and overheads, the lower bound of the energy consumption per information bit can be further tightened as

$$E_b \geq \left(\frac{P_r+P_{\text{SYN}}+\rho_t E_p R_p}{1/D_s}\right) N\frac{T_{\text{on}}+2T_{\text{IPS}}+T_{\text{ACK}}}{T_{\text{onL}}}, \tag{15}$$

where $N$ is the total number of transmissions. $(T_{\text{on}}+2T_{\text{IPS}}+T_{\text{ACK}})/T_{\text{onL}}$ denotes the rate penalty caused by packetization, where $T_{\text{IPS}}$ denotes inter packet space and $T_{\text{ACK}}$ represents the time duration the transmitter listens for acknowledgement from the receiver. The detailed formulas of $T_{\text{IPS}}$ and $T_{\text{ACK}}$ can be found in the following section. The above parameters are determined by the detailed packet structure, channel conditions, and modulation schemes. Although (15) implies an ideal wideband channel with no multipath and omits the possible energy losses due to circuit start-up, this model tightens the bound from (12) and better represents practical scenarios since both $N$ and $(T_{\text{on}}+2T_{\text{IPS}}+T_{\text{ACK}})/T_{\text{onL}}$ are greater than or equal to 1.

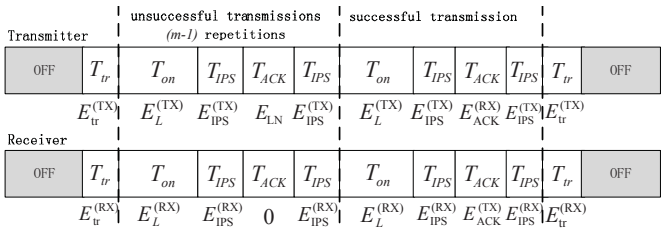


Fig. 2. The transmission and reception of one packet using $N$ total transmissions.

### *B. Practical Average Energy Consumption Per Information Bit*

Although (15) provides a lower bound on the energy consumption per information bit, it does not consider many practical issues. For example, it does not consider the energy spent on the packet overhead and listening. In practice, we need to consider the detailed procedure of transmitting one packet instead of one bit [7].

*1) Energy Consumption per Packet with Retransmissions:* To guarantee the successful reception of one packet, an automatic repeat request (ARQ) protocol is used. A delivery procedure involving $N-1$ retransmissions is shown in Fig. 2. The inter packet space (IPS) is denoted by $T_{\text{IPS}}$. The power consumption during $T_{\text{IPS}}$ is mainly due to the clock generator and synchronizer. Therefore, the corresponding energy consumption at the transmitter is $E_{\text{IPS}}^{(\text{TX})} = P_{\text{SYN}}T_{\text{IPS}}$, while the receiver consumes $E_{\text{IPS}}^{(\text{RX})} = \rho_r P_{\text{SYN}}T_{\text{IPS}}$.

We assume that before transmission or reception of a packet, the transmitter and receiver spend $T_{\text{tr}}$ amount of time to go from the off (sleep) state to an on (active) state. We refer to this time duration as the "transient session". During the transient session, the transmitter consumes $E_{\text{tr}}^{(\text{TX})} = P_{\text{SYN}}T_{\text{tr}}$ amount of energy to start the front end clock generator and synchronizer. Similarly, the receiver consumes $E_{\text{tr}}^{(\text{RX})} = \rho_r P_{\text{SYN}}T_{\text{tr}}$.

$T_{\text{on}}$ is the time duration for the transmission of one packet. That is

$$\begin{aligned}T_{\text{on}} &= T_{\text{SP}}+T_{\text{PHR}}+T_{\text{onL}}, \\ &= (L_{\text{SP}}+\tfrac{L_{\text{PHR}}}{R_c})/R_{\text{base}}+\tfrac{L_L}{R_b R_c}.\end{aligned} \tag{16}$$

The energy consumptions at the transmitter and receiver during $T_{\text{on}}$ are

$$\begin{aligned}E^{(\text{TX})} &= E_L^{(\text{TX})}+E_O^{(\text{TX})}, \\ E^{(\text{RX})} &= E_L^{(\text{RX})}+E_O^{(\text{RX})}.\end{aligned} \tag{17}$$

where $E_L^{(\text{TX})}$, $E_O^{(\text{TX})}$, $E_L^{(\text{RX})}$ and $E_O^{(\text{RX})}$ are given in (3), (4), (5) and (6), respectively.

$T_{\text{ACK}}$ is the time period when the transmitter listens for an acknowledgement. We set $T_{\text{ACK}} = T_O$. Overall, the definitions of the energy consumptions within one transmission are summarized as follows

$$\begin{aligned} E_{\text{IPS}} &= 2E_{\text{IPS}}^{(\text{TX})} + 2E_{\text{IPS}}^{(\text{RX})}, \\ E_{\text{LN}} &= \rho_r P_{\text{SYN}} T_{\text{ACK}}, \\ E_{\text{TRAN}} &= 2E_{\text{tr}}^{(\text{TX})} + 2E_{\text{tr}}^{(\text{RX})}, \\ E_{\text{ACK}}^{(\text{RX})} &= P_r T_{\text{ACK}}, \\ E_{\text{ACK}}^{(\text{TX})} &= (L_{\text{SP}} + L_{\text{PHR}}/R_c)E_p + P_{\text{SYN}} T_{\text{ACK}}, \\ E^{(\text{TX})} &= E_L^{(\text{TX})} + E_O^{(\text{TX})}, \\ E^{(\text{RX})} &= E_L^{(\text{RX})} + E_O^{(\text{RX})}, \end{aligned} \tag{18}$$

where $E_{\text{IPS}}$ is the total energy consumed by the receiver and the transmitter in IPSs within one transmission. $E_{\text{TRAN}}$ is the total energy consumption of the receiver and the transmitter during the transient sessions. In both IPSs and transient sessions, only the frequency synthesizers consume energy.

$E_{\text{LN}}$ denotes the energy consumption of the transmitter on listening to the media for the ACK from the receiver in the first $N-1$ unsuccessful transmissions. Therefore, $E_{\text{LN}}$ is the energy consumption of idle listening during $T_{\text{ACK}}$. $E_{\text{ACK}}^{(\text{RX})}$, $E_{\text{ACK}}^{(\text{TX})}$ are the energy consumption of the transmitter for receiving the ACK and the energy consumption of the receiver for transmitting the ACK. In this paper, we assume the ACK message is simply a packet containing only the PHR and the SP. Since the PHR and the SP always consist of $\{-1, 1\}$ symbols and only coherent detection with SD combining is used, $E_{\text{ACK}}^{(\text{RX})}$ and $E_{\text{ACK}}^{(\text{TX})}$ are constant for a given repetition coding scheme.

The decomposition of the energy consumption during each packet transmission session has been shown in Section IV-B1. Therefore, the average energy consumption for successful delivery of a packet can be expressed as

$$\begin{aligned} E &= (E^{(\text{TX})} + E^{(\text{RX})} + E_{\text{LN}} + E_{\text{IPS}})N \\ &\quad - E_{\text{LN}} + E_{\text{TRAN}} + E_{\text{ACK}}^{(\text{TX})} + E_{\text{ACK}}^{(\text{RX})}, \end{aligned} \tag{19}$$

where $N$ is the average number of transmissions/receptions required to successfully deliver one packet. The average number of transmissions $N = 1/(1-P_b)^{L_L}$, where $P_b$ is the average BEP. Note that $(1-P_b)^{L_L}$ is the probability that a packet is received correctly. As shown in the following subsection, the average BEP $P_b$ is closely related to the modulation type, detection schemes, repetition coding/combing schemes, and number of Rake fingers.

*2) Average BEP over Independent Nakagami Fading Channels:* The average BEP can be obtained utilizing the characteristic function of the pdf of the output SNR after the MRC [30][31][32]. The instantaneous SNR at the *i*th finger is

$$\gamma_i = \frac{|\alpha_i|^2 P_{\text{tx}}}{G_d \sigma^2}, \tag{20}$$

where $P_{\text{tx}}$ is the transmit power, $G_d$ denotes the path loss at distance $d$, and $\sigma^2$ represents the noise power at the receiver. Also, $\alpha_i$ represents the attenuation of the selected path preserving the *i*th largest power. The instantaneous SNR at the output of the MRC is $\gamma = \sum_{i=1}^{M} \gamma_i$.

The average bit error probability of DBPSK-CO can be found by averaging the BEP of DBPSK-CO over an AWGN channel, with the pdf of $\gamma$ which is indicated by $p(\gamma)$. By using an alternate representation of the Q-function, we have the BEP of DBPSK-CO over an AWGN channel as [33][34]

$$\begin{aligned} P_{b,\text{DBPSK-CO,AWGN}} &\approx 2Q(\sqrt{2\gamma})[1 - Q(\sqrt{2\gamma})]. \\ &\approx 2Q(\sqrt{2\gamma}), \\ &= \tfrac{2}{\pi}\int_0^{\frac{\pi}{2}} e^{-\frac{2\gamma}{\sin^2\phi}} d\phi. \end{aligned} \tag{21}$$

The average BEP can be expressed as

$$\begin{aligned} P_{b,\text{DBPSK-CO}} &= \int_0^{\infty} P_{b,\text{DBPSK-CO,AWGN}} p(\gamma) d\gamma, \\ &= \int_0^{\infty} \left\{ \tfrac{2}{\pi}\int_0^{\frac{\pi}{2}} e^{-\frac{2\gamma}{\sin^2\phi}} d\phi \right\} p(\gamma) d\gamma, \\ &= \tfrac{2}{\pi}\int_0^{\frac{\pi}{2}} \left\{ \int_0^{\infty} e^{-\frac{2\gamma}{\sin^2\phi}} p(\gamma) d\gamma \right\} d\phi, \\ &= \tfrac{2}{\pi}\int_0^{\frac{\pi}{2}} \left\{ \int_0^{\infty} e^{-\frac{2\gamma}{\sin^2\phi}} p(\gamma) d\gamma \right\} d\phi. \end{aligned} \tag{22}$$

On the other hand, the moment generating function (MGF) of the pdf of $\gamma$ is defined as $\Psi_\gamma(\nu) = \int_0^{\infty} e^{\nu\gamma} p(\gamma) d\gamma$. Therefore,

$$P_{b,\text{DBPSK-CO}} = \frac{2}{\pi}\int_0^{\frac{\pi}{2}} \Psi_\gamma(\nu)|_{\nu = -\frac{2}{\sin^2\phi}} d\phi. \tag{23}$$

Since $\alpha_{k,l}$ follows a Nakagami-m distribution from the channel model, the MGF of the pdf of $\gamma$ has been established as [30]

$$\Psi_\gamma(\nu) = \prod_{i=1}^{M} \frac{1}{(1 - \nu\bar{\gamma}_i/m_i)^{m_i}} \tag{24}$$

where $\bar{\gamma}_i = \mathbf{E}[|\alpha_i|^2] P_{\text{tx}} G_c / G_d \sigma^2$ is the average received SNR at the *i*th finger. $\mathbf{E}[|\alpha_i|^2]$ represents the average power of the *i*th selected path, that is $\mathbf{E}[|\alpha_i|^2] = \mathbf{E}[|\alpha_{k,l}|^2]$, where $|\alpha_{k,l}|^2$ has the *i*th largest expectation among all paths. $m_i$ is the Nakagami m-factor for the *i*th selected path. As shown in [26], for the first ray of each cluster, $m_i$ is assumed to be deterministic and independent of delay; while for the remaining paths, $m_i$ follows a delay-dependence lognormal distribution.

Moreover, if we consider repetition coding with parameter $N_p$ and SD combining, the average SNR will increase $N_p$ times compared with the corresponding uncoded modulations. That is, the eventual average BEP for DBPSK with coherent detection and SD combining (DBPSK-CO-SD) is

$$P_{b,\text{DBPSK-CO-SD}} = \tfrac{2}{\pi}\int_0^{\frac{\pi}{2}} \Psi_\gamma(\nu)\big|_{\nu = -\frac{2N_p}{\sin^2\phi}} d\phi. \tag{25}$$

Instead, if HD combining is used, the average BEP for DBPSK with coherent detection and HD combining (DBPSK-CO-HD) $P_{b,\text{DBPSK-CO-HD}}$ can be expressed ass

$$\begin{aligned} &P_{b,\text{DBPSK-CO-HD}} \\ &= \sum_{k=\frac{N_p+1}{2}}^{N_p} \binom{N_p}{k} P_{b,\text{DBPSK-CO}}^{k} (1 - P_{b,\text{DBPSK-CO}})^{N_p - k}, \end{aligned} \tag{26}$$

where $P_{b,\text{DBPSK-CO}}$ is given in (22). A similar procedure can be directly applied to OOK with coherent detection and DPPM with coherent detection, using either HD or SD combining.

In the case of DBPSK-NC, the average bit error probability of DBPSK-CO can be found by directly utilizing the MGF of

the pdf of $\gamma$. First, we have the BEP of DBPSK-NC over an AWGN channel as [34]

$$P_{b,\text{DBPSK-NC,AWGN}} \approx \tfrac{1}{2}e^{-\gamma} \tag{27}$$

The average BEP can then be expressed as

$$\begin{aligned} P_{b,\text{DBPSK-NC}} &= \int_0^\infty P_{b,\text{DBPSK-NC,AWGN}} p(\gamma) d\gamma, \\ &= \int_0^\infty \tfrac{1}{2} e^{-\gamma} p(\gamma) d\gamma, \\ &= \tfrac{1}{2}\Psi_\gamma(\nu)|_{\nu=-1}, \\ &= \tfrac{1}{2}\prod_{i=1}^{M} \tfrac{1}{(1+\bar{\gamma}_i/m_i)^{m_i}} \end{aligned} \tag{28}$$

Correspondingly, we have

$$P_{b,\text{DBPSK-NC-SD}} = \frac{1}{2}\prod_{i=1}^{M} \frac{1}{\left(1+N_p\bar{\gamma}_i/m_i\right)^{m_i}}, \tag{29}$$

and

$$\begin{aligned} &P_{b,\text{DBPSK-NC-HD}} \\ &= \sum_{k=\frac{N_p+1}{2}}^{N_p} \binom{N_p}{k} P_{b,\text{DBPSK-NC}}^{k} (1-P_{b,\text{DBPSK-NC}})^{N_p-k}. \end{aligned} \tag{30}$$

The average bit error probabilities of DPPM and OOK with non-coherent detection, using either HD or SD combing, can be obtained following a similar procedure. Moreover, to avoid excessive requirements of memory units, only HD combining is considered for noncoherent detections.

*3) Energy per Information Bit Minimization:* From (19), the energy consumption per information bit is

$$\begin{aligned} E_b &= \frac{(E^{(\text{TX})}+E^{(\text{RX})}+E_{\text{LN}}+E_{\text{IPS}})}{L_L(1-P_b)^{L_L}} \\ &\quad + \frac{E_{\text{TRAN}}+E_{ACK}^{(\text{TX})}+E_{\text{ACK}}^{(\text{RX})}-E_{\text{LN}}}{L_L}. \end{aligned} \tag{31}$$

Our goal is to find an optimum combination of the modulation scheme, the detection scheme, the repetition coding parameter $N_p$, the combining scheme, the packet length, $L_L$, and the number of RAKE fingers at the receiver, $M$, over a slow frequency-selective channel for a given transmission distance, that minimizes the effective energy consumption per information bit denoted by (31). Removing the integer constraint on $L_L$, it is straight forward to find the closed form optimum packet length by solving $\partial E_b/\partial L_L = 0$. At high SNR, the result is

$$L_L^* \approx \frac{-P_b(A+B)+\sqrt{P_b^2(A+B)^2+4(A+B)CP_b}}{2CP_b}, \tag{32}$$

where

$$\begin{aligned} A &= E_{\text{TRAN}} + E_{ACK}^{(\text{TX})} + E_{\text{ACK}}^{(\text{RX})} - E_{\text{LN}}, \\ B &= E_{\text{IPS}} + E_{\text{LN}} + E_O^{(\text{TX})} + E_O^{(\text{RX})} + E_L^{(\text{RX})}, \\ C &= (\rho_t E_p + P_{\text{SYN}}/R_b)/R_c \\ &\quad + [\rho_t(MP_{\text{COR}} + \rho_c P_{\text{ADC}} + P_{\text{LNA}} + P_{\text{VGA}}) \\ &\quad + \rho_r(P_{\text{GEN}} + P_{\text{SYN}})]/(R_b R_c). \end{aligned}$$

As indicated by (32), $L_L^*$ will decrease as BEP increases. In a real application of this model, the packet length can always be selected as the nearest integer of the resulting $L_L^*$.

In this paper, we have assumed that the data rate is fixed at the maximum allowable data rate that avoids ISI. Correspondingly, the transmit power, as shown in (1), is also fixed. Therefore, the average BEP at a given transmission distance for a given modulation scheme is only determined by the modulation and detection schemes, repetition coding and combining schemes, and the number of RAKE fingers at the receiver. For a given combination of the modulation/detection scheme and the repetition coding/combining scheme, the BEP follows a non-increasing function of the number of RAKE fingers. Thus, $L_L^*$ follows a non-decreasing function of the number of RAKE fingers.

The optimum number of RAKE fingers reflects the tradeoff between the power consumption cost, $MP_{\text{COR}}$ and the received power gain, $\mathbf{E}[|\alpha_i|^2]P_{\text{tx}}/G_d$. The optimum selection of modulation/detection schemes and repetition coding/combining schemes reflects the tradeoff between the performance and the power consumption at the transceiver, since higher performance is often accompanied by higher power consumption. Unlike the optimum packet length, there are no closed form expressions for the optimum modulation/detection schemes, repetition coding/combining schemes and number of RAKE fingers. However, numerical optimizations can be performed over these parameters, and the optimization results will be given in the following section.

## V. Numerical Results

In this section, we demonstrate the results of minimizing the effective energy consumption per information bit modeled by equation (31). We assume that $B = 500$ MHz, $L_{\text{SP}} = 1024$ symbols, $L_{\text{PHR}} = 16$ symbols [1], coding rate $R_c = 1/N_p$, and $N_p = 1, 3, 5, ..., 15$. The maximum excess delay is $D_S = 40$ ns, which limits the maximum pulse rate to $R_p \approx 1/D_s = 25$ Mbps to avoid inter symbol interference. The power consumptions of the transmitter and receiver components are as follows [28],[35]-[38]: $P_{\text{SYN}} = 30.6$ mW, $P_{\text{ADC}} = 2.2$ mW, $P_{\text{GEN}} = 2.8$ mW, $P_{\text{VGA}} = 22$ mW, $P_{\text{LNA}} = 9.4$ mW, $P_{\text{COR}} = 10.08$ mW. To the best of our knowledge, there is no existing literature providing specific power consumption evaluations of the channel estimation block in an IR-UWB receiver. Therefore, in this paper we assume the IR-UWB receiver uses the data-aided estimation method from [39], which can essentially be implemented as a correlator. Thus, we assume $P_{\text{EST}} = P_{\text{COR}} = 10.08$ mW.

The fixed emitted energy per pulse is $E_p = 4.5$ pJ/pulse. Therefore, the maximum amount of transmit power is $P_{\text{tx}} = E_p R_p = 0.113$ mW. Also, we assume $T_{\text{IPS}} = 200$ $\mu$s and $T_{\text{tr}} = 400$ $\mu$s. Moreover, $R_{\text{base}} = 1$ Mbps, where $R_{\text{base}}$ denotes the data rate to transmit the header and preamble symbols, and the path loss parameter is set to $L_w = 0.7$ dB/m.

The parameters of the channel model for an office environment with no line of sight (NLOS) are used [26]. That is, the path loss exponent $n = 3.07$, the frequency dependency decaying factor $\kappa = 0.71$, reference path gain $G_0 = -59.9$ dB, transmission center frequency $f = 3.1$ GHz, the reference frequency $f_c = 5$ GHz. The distance range of interest is $d \in [3, 27]$ meters. We used exhaustive search to solve the optimization model. The quality of service (QoS) is assumed to be error free. That is, the expected number of total transmissions is $1/(1-P_b)^{L_L}$.

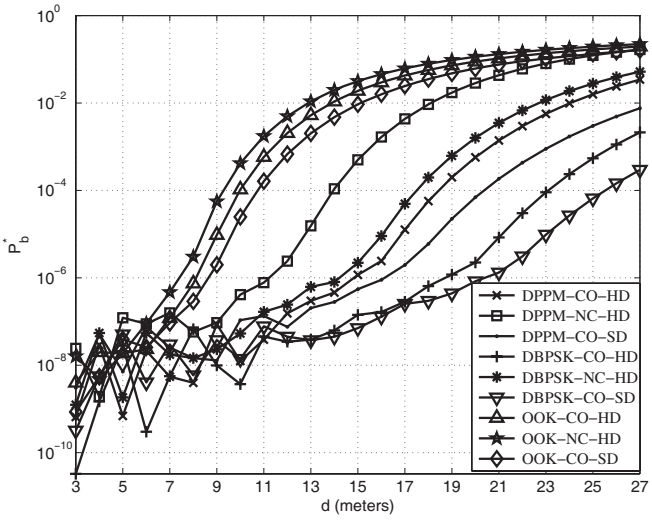


Fig. 3. The optimum target BEP versus distance ($N_p = 3$).

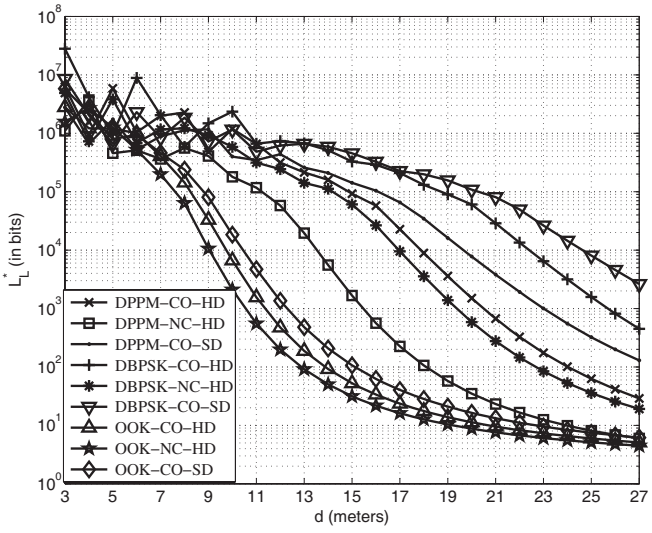


Fig. 4. The optimum packet length versus distance ($N_p = 3$).

### A. Optimization with Fixed $N_p$

To better understand the influence of the packet length, the number of RAKE fingers, and the modulation/combining/detection schemes, first, we consider a fixed $N_p = 3$ to isolate the impact of repetition coding from the rest of the parameters.

The optimum BEPs and optimum packet lengths of different modulation/combining/detection schemes with $N_p = 3$ are shown in Figs. 3 and 4, respectively. As shown in Fig. 3, as the transmission distance increases, the optimum BEP will increase since it will require increasingly more power at the receiver to maintain a low BEP as $d$ increases. Therefore, the optimum choice is to lower the target BEPs to avoid a dramatic increase in the number of RAKE fingers. Correspondingly, as shown in Fig. 4, the optimum packet length will decrease as $d$ increases to avoid costly retransmissions caused by higher BEP, since a short packet length results in a lower packet error probability.

Note that, at short transmission distances, there are high variations of $P_b^*$ and $L_L^*$. This is because at short distances

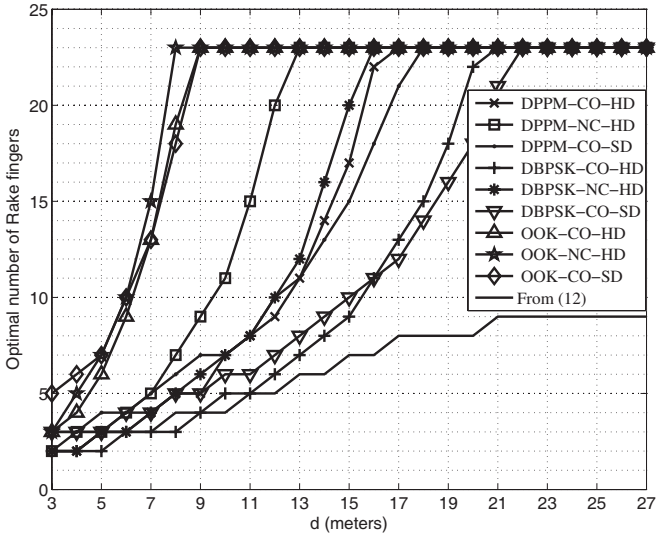


Fig. 5. The optimum number of RAKE fingers versus distance ($N_p = 3$).

where $P_b^*$ is very low, $P_b^*$ is very sensitive to a change in the number of RAKE fingers. That is, at short distances, additional RAKE fingers will provide a considerable amount of collected power gain. Correspondingly, $L_L^*$ will change significantly as the number of RAKE fingers changes at short distances. On the other hand, at large distances, additional RAKE fingers only provide a small amount of collected power gain. Therefore, $P_b^*$ and $L_L^*$ are not sensitive to a change in the number of RAKE fingers. The curves of $P_b^*$ and $L_L^*$ thereby become smooth as distances increase.

Fig. 5 shows the optimum number of RAKE fingers at the receiver versus distance. As the transmission distance increases, the optimum number of RAKE fingers will increase and converge to a certain value. This is due to the change of balance between the diversity gain and the power cost induced by each additional RAKE finger. The absolute value of the increase in collected energy by an additional RAKE finger decreases with distance. This diminishing gain incurs a fixed cost, namely $P_{\text{COR}}$. Consequently, as distance increases, to avoid excessive retransmissions, the number of RAKE fingers should increase to collect more received power. However, when distance increases beyond a certain level, path loss becomes very large, and increasing the number of RAKE fingers does not lead to the collection of considerably more received power. However, more RAKE fingers will incur more power consumption at the receiver. Thus, at large transmission distances, increasing the number of RAKE fingers does not improve the energy efficiency. The optimum receiver power consumptions of different modulation schemes at different transmission distances follow the trend of the optimum number of RAKE fingers shown in Fig. 5. The optimum number of RAKE fingers from (12) is also shown in Fig. 5. Since (12) does not include the imperfection of repetition coding/modulation and the overhead caused by packetization and retransmissions, the received power that is collected by the RAKE fingers at the receiver reaches the theoretical maximum efficiency (no waste on overhead).

The overall minimized energy consumption per information

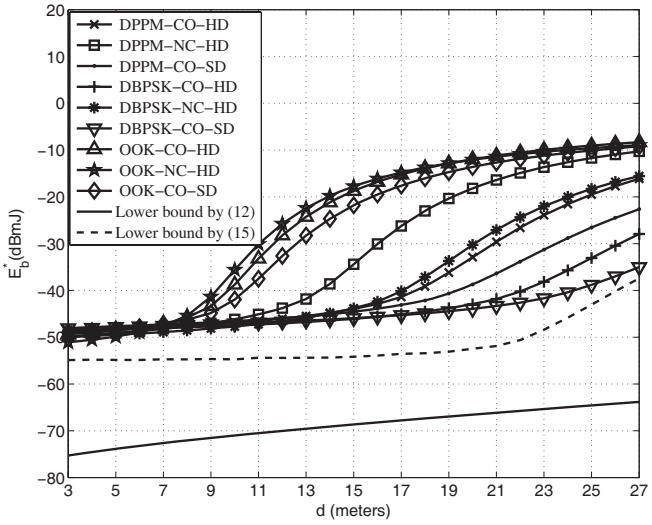


Fig. 6. The minimum energy consumption per information bit versus distance ($N_p = 3$).

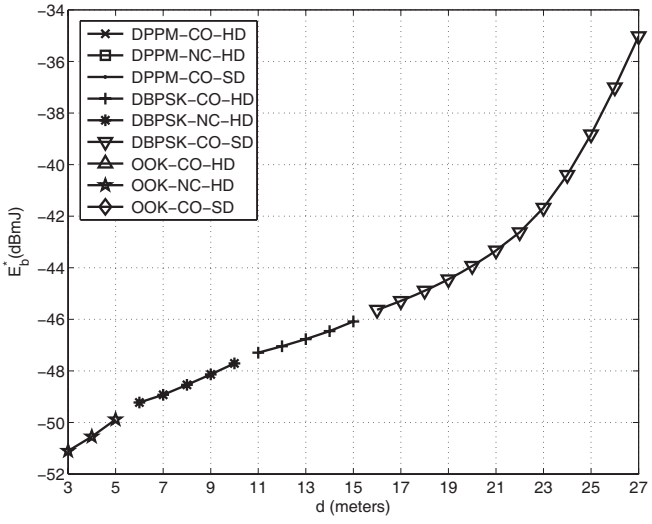


Fig. 7. The overall minimum energy consumption per information bit and corresponding modulation/decoding/detection schemes ($N_p = 3$).

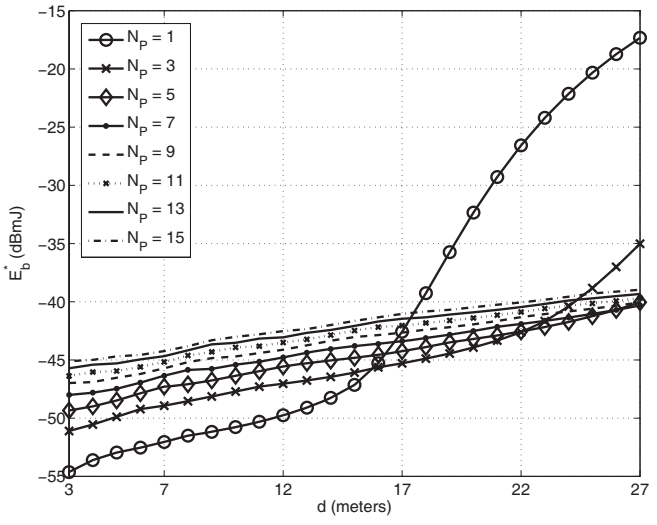


Fig. 8. The overall minimum energy consumption per information bit for different repetition coding parameters with optimized $L_L$, $M$, and modulation/repetition coding/detection schemes.

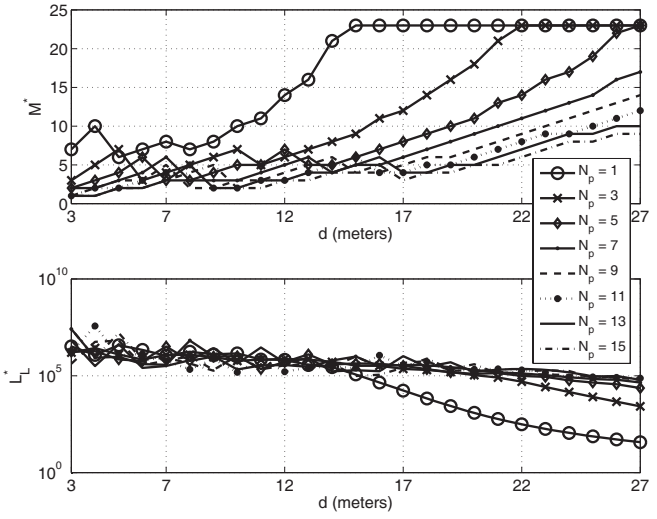


Fig. 9. The $M^*$ and $L_L^*$ with optimized modulation/combining/detection schemes for different $N_p$.

bit is shown in Fig. 6. OOK-NC-HD consumes the least amount of energy when $d < 6$m, while DBPSK-NC-HD offers the lowest energy consumption per information bit when $6\text{m} \leq d < 11\text{m}$. DBPSK-CO-HD is the most energy efficient scheme when $11\text{m} \leq d < 16\text{m}$. DBPSK-CO-SD is the most energy efficient scheme when the distance is greater than 16 meters. This trend reflects the balance between the transmitter energy consumption and the receiver energy consumption. At a short transmission distance, the less robust schemes (OOK-NC-HD) require less power consumption at the transmitter/receiver and provide a BEP low enough to avoid excessive retransmissions. Therefore, the OOK scheme, noncoherent detection, and HD combining have a high energy efficiency at short transmission distances. However, as transmission distance increases, the above schemes require a large number of RAKE fingers to maintain a low BEP, thereby the receiver power consumption will increase dramatically if using schemes like OOK-NC-HD. On the other hand, the more robust schemes (such as DBPSK-CO-HD, DBPSK-CO-SD) consume much less power at the receiver since they need fewer RAKE fingers to achieve a low BEP. Thus, as transmission distance increases, these schemes will become the energy efficient schemes. The lower bound on $E_b$ from (12) and the packetized lower bound on $E_b$ from (15) are also shown in Fig. 6. The packetized bound from (15) is larger than (12), especially for large distances. This is caused by the decrease of $L_L^*$ as distance increases, as shown in Fig. 4, which in turn increases the packetization overhead.

The overall minimum $E_b$ and corresponding modulation, repetition coding and detection schemes are shown in Fig. 7. This figure, together with Fig. 5, reveals that, at short distances (high SNRs), low complexity and low performance modulation/repetition coding/detection schemes, such as OOK-NC-HD with a small number of RAKE fingers, are energy efficient; while at large distances (low SNRs), higher complexity and higher performance modulation/repetition coding/detection schemes, such as DBPSK-CO-SD with a large number of RAKE fingers, become energy efficient.

TABLE I
OVERALL OPTIMUM CONFIGURATIONS

| Distance (m) | Modulation | Detection | $N_p$ | Combining | $M^*$ | $L_L^*$ (Kbit) |
|---|---|---|---|---|---|---|
| 3 | OOK | NC | 1 | HD | 7 | $\sim 1500$ |
| 4 | | | | | 10 | |
| 5 | DBPSK | | | | 6 | |
| 6 | | | | | 7 | |
| 7 | | | | | 8 | |
| 8 | | CO | | | 7 | |
| 9 | | | | | 8 | |
| 10 | | | | | 10 | |
| 11 | | | | | 11 | $\sim 500$ |
| 12 | | | | | 14 | |
| 13 | | | | | 16 | |
| 14 | | | | | 21 | |
| 15 | | | | | 23 | |
| 16 | | | 3 | SD | 12 | |
| 17 | | | | | 14 | |
| 18 | | | | | 16 | |
| 19 | | | | | 18 | |
| 20 | | | | | 21 | |
| 21 | | | | | 23 | $\sim 50$ |
| 22 | | | 5 | | 16 | |
| 23 | | | | | 17 | |
| 24 | | | | | 19 | |
| 25 | | | 7 | | 16 | |
| 26 | | | | | 17 | |
| 27 | | | | | 19 | |

### *B. Optimization with Variable $N_p$*

Besides the optimization on packet length, number of RAKE fingers and modulation/combining/ detection schemes, the repetition coding parameter $N_p$ in repetition coding should also be adjusted to minimize $E_b$. Now we assume that $N_p$ takes the values $1, 3, 5, ..., 15$.

Fig. 8 shows the overall minimum energy consumption per information bit for different repetition coding parameters. To show the influence of $N_p$, the $E_b^*$ shown in Fig. 8 have been optimized over $L_L$, $M$ and modulation/repetition coding/detection schemes. Fig. 8 shows that the optimum $N_p$ increases as $d$ increases (SNR decreases). This observation further confirms that, to guarantee link level reliable communication, high-complexity and high-performance transceiver structures are energy efficient at low SNRs; while low-complexity and low-performance transceiver structures are energy efficient at high SNRs.

Fig. 9 shows the optimum number of RAKE fingers and packet lengths for different repetition coding parameters $N_p$, with optimized modulation/combining/detection schemes. The curves with different $N_p$ display the same trend: as $d$ increases (SNR decreases), $M^*$ increases and converges to the same level, while $L_L^*$ decreases. Fig. 9 also reveals that the effect of a large $N_p$ on the packet error probability on the expected number of retransmissions is equivalent to that of a small $L_L$ or a large $M$, and vice versa. Therefore, it is possible to use a long repetition code to minimize energy under some circumstances where a large number of RAKE fingers and adjustable packet lengths are not feasible.

### *C. Optimum Configuration Table*

The results of these optimizations can enable the transceiver to adapt by selecting the overall optimum configurations (including the modulation/detection scheme, the repetition coding/combining scheme, the packet length and the number of RAKE fingers) according to the expected transmission distance through a lookup table. Table I is an example of such a look-up table obtained with the particular power consumption and channel models assumed in this paper.

### *D. The Effects of Power Consumption Values on the Optimum Configurations*

Implementation technologies have a paramount impact on the choice of the optimal communication schemes. For example, should $P_{\text{SYN}}$ become smaller, the distance range in which coherent detection is energy efficient becomes larger. In fact, considering an extreme case where the transceiver does not consume any power, we shall always use the communication scheme with the highest performance, such as DBPSK with coherent detection, soft decoding and an all-RAKE receiver. In real applications, the overall optimum configurations should be carefully evaluated using the generic energy consumption model provided in this paper as summarized in (31) and the power consumption values of the actual circuit components based on the adopted production technologies. For instance, suppose we choose another set of power consumption values where $P_{\text{SYN}} = 2.2$ mW, while the rest of the power consumption values stay the same. The resulting overall optimum configurations are summarized in Table II. By comparing

TABLE II
OVERALL OPTIMUM CONFIGURATIONS

| Distance (m) | Modulation | Detection | $N_p$ | Combining | $M^*$ | $L_L^*$ (Kbit) |
|---|---|---|---|---|---|---|
| 3 | OOK | NC | 1 | HD | 7 | $\sim 3000$ |
| 4 | | CO | | | 9 | $\sim 1500$ |
| 5 | DBPSK | | | | 4 | |
| 6 | | | | | 5 | |
| 7 | | | | | 6 | |
| 8 | | | | | 7 | |
| 9 | | | | | 8 | |
| 10 | | | | | 9 | $\sim 500$ |
| 11 | | | | | 11 | |
| 12 | | | | | 13 | |
| 13 | | | | | 15 | $\sim 100$ |
| 14 | | | | | 18 | |
| 15 | | | | | 22 | |
| 16 | | | 3 | SD | 10 | |
| 17 | | | | | 11 | |
| 18 | | | | | 12 | |
| 19 | | | | | 14 | |
| 20 | | | | | 16 | |
| 21 | | | 5 | | 18 | $\sim 50$ |
| 22 | | | | | 13 | |
| 23 | | | | | 14 | |
| 24 | | | | | 16 | |
| 25 | | | | | 18 | |
| 26 | | | 7 | | 14 | |
| 27 | | | | | 16 | |

Tables I and II, we find that since the difference in power consumption of coherent and noncoherent schemes becomes smaller, the distance range in which coherent detection is energy efficient becomes larger. However, the general trend of the optimal configurations versus transmission distance stays the same: high-complexity and high-performance transceiver structures are energy efficient at large distances; while low-complexity and low-performance transceiver structures are energy efficient at short distances.

## VI. CONCLUSIONS

In this paper, we provided the power consumption models of typical transmitter and receiver structures of IR-UWB systems. Then, under the assumption of a frequency selective time-invariant channel, we determine the optimum combination of the modulation scheme, the detection scheme, the repetition coding parameter, the combining scheme, the packet length, and the number of RAKE fingers at the receiver to minimize energy consumption per information bit. An optimum number of RAKE fingers exists under the assumption of a frequency selective time-invariant channel with a double exponentially decaying power delay profile. The results show that low-complexity, low-performance transmission schemes are energy efficient at high SNRs, while high-complexity, high-performance schemes are energy efficient at low SNRs. Using the specific power consumption values selected in this paper, we provided detailed optimum transmission schemes, including packet length, modulation, detection, repetition coding, combining, and number of RAKE fingers for given transmission distances for a typical IR-UWB link.

## REFERENCES

[1] F. C. Commission, "Part 15 of the Commission's Rules Regarding Ultra-Wideband Transmission Systems Federal Communications Commission," July 2008.

[2] I. Gresham, A. Jenkins, R. Egri, C. Eswarappa, N. Kinayman, N. Jain, R. Anderson, F. Kolak, R. Wohlert, S. Bawell, J. Bennett, and J. Lanteri, "Ultra-wideband radar sensors for short-range vehicular applications," *IEEE Trans. Microwave Theory and Techniques*, vol. 52, pp. 2105–2122, Sep. 2004.

[3] S. Gezici, T. Zhi, G. Giannakis, H. Kobayashi, A. Molisch, H. Poor, and Z. Sahinoglu, "Localization via ultra-wideband radios: a look at positioning aspects for future sensor networks," *IEEE Signal Process. Mag.*, vol. 22, pp. 70–84, July 2005.

[4] I. Oppermanz, L. Stoica, A. Rabbachin, Z. Shelby, and J. Haapola, "UWB wireless sensor networks: UWEN - a practical example," *IEEE Commun. Mag.*, vol. 42, pp. S27–S32, Dec. 2004.

[5] A. J. Goldsmith and S. B. Wicker, "Design challenges for energy-constrained ad hoc wireless networks," *IEEE Wireless Commun.*, Aug. 2002.

[6] I. Akyildiz, S. Weilian, Y. Sankarasubramaniam, and E. Cayirci, "A survey on sensor networks," *IEEE Commun. Mag.*, vol. 40, pp. 102–114, Aug. 2002.

[7] T. Wang, W. Heinzelman, and A. Seyedi, "Minimization of transceiver energy consumption in wireless sensor networks with AWGN channels," in *Proc. Allerton Conference*, Sep. 2008.

[8] S. Cui, A. J. Goldsmith, and A. Bahai, "Energy-constrained modulation optimization," *IEEE Trans. Wireless Commun.*, vol. 4, no. 8, pp. 2349–2360, Sep. 2005.

[9] M. Z. Win and R. A. Scholtz, "On the energy capture of ultrawide bandwidth signal in dense multipath environments," *IEEE Commun. Lett.*, vol. 2, no. 9, 1998.

[10] D. Cassioli, M. Z. Win, F. Vatalaro, and A. F. Molisch, "Low complexity Rake receivers in ultra-wideband channels," *IEEE Trans. Wireless Commun.*, vol. 4, pp. 1265–1275, Apr. 2007.

[11] T. Wang, W. Heinzelman, and A. Seyedi, "Minimizing energy consumption in IR-UWB based wireless sensor networks," in *Proc. IEEE International Conference on Communications (ICC)*, June 2009.

[12] S. Cui, A. J. Goldsmith, and A. Bahai, "Energy-efficiency of MIMO and cooperative MIMO techniques in sensor networks," *IEEE J. Sel. Areas Commun.*, vol. 22, no. 6, pp. 1089–1098, Aug. 2004.

[13] J. Ammer and J. Rabaey, "The energy-per-useful-bit metric for evaluating and optimizing sensor network physical layers," *3rd Annual IEEE Communications Society on Sensor and Ad Hoc Communications and Networks (SECON '06)*, Sep. 2006.

[14] X. Lu, E. Erkip, Y. Wang, and D. Goodman, "Power efficient multimedia communication over wireless channels," *IEEE J. Sel. Areas Commun.*, vol. 21, no. 10, pp. 1738–1751, Dec. 2003.

[15] P. Lettieri and M. B. Srivastava, "Adaptive frame length control for improving wireless link throughput, range, and energy efficiency," in *Proc. INFOCOM '98*, Mar. 1998.

[16] Y. Sankarasubramaniam, I. Akyildiz, and S. McLaughlin, "Energy efficiency based packet size optimization in wireless sensor networks," in *Proc. First IEEE 2003 IEEE International Workshop on Sensor Network Protocols and Applications*, 2003.

[17] S. Cui, A. J. Goldsmith, and A. Bahai, "Exact bit error rate analysis of TH-PPM UWB systems in the presence of multiple-access interference," *IEEE Commun. Lett.*, vol. 7, no. 12, pp. 572–574, Dec. 2003.

[18] Q. Zhang and J. H. Cho, "On RAKE receivers for ultra-wideband binary block-coded PPM in dense multipath channels," *IEEE Trans. Veh. Technol.*, vol. 56, no. 4, pp. 1737–1747, July 2007.

[19] J. D. Choi and W. E. Stark, "Performance of ultra-wideband communications with suboptimal receivers in multipath channels," *IEEE J. Sel. Areas Commun.*, vol. 20, no. 9, pp. 1754–1766, Dec. 2002.

[20] N. Telzhensky and Y. Leviatan, "Novel method of UWB antenna optimization for specified input signal forms by means of genetic algorithm," *IEEE Trans. Antennas Propag.*, vol. 54, no. 8, pp. 2216–2225, Aug. 2006.

[21] R. Zhang and X. Dong, "Synchronization and integration region optimization for UWB signals with non-coherent detection and autocorrelation detection," *IEEE Trans. Commun.*, vol. 54, no. 5, pp. 790–798, May 2008.

[22] Y. Shi, Y. T. Hou, and H. D. Sherali, "Cross-layer optimization for data rate utility problem in UWB-based ad hoc networks," *IEEE Trans. Mobile Computing*, vol. 7, no. 6, pp. 764–777, June 2008.

[23] U. Onunkwo and Y. Li, "On the optimum pulse-position modulation index for ultra-wideband communication," Shanghai, China, June 2004, pp. 77–80.

[24] M. Z. Win and R. A. Scholtz, "On the energy capture of ultrawide bandwidth signals in dense multipath environments," *IEEE Commun. Lett.*, vol. 2, no. 9, pp. 245–247, Sep. 1998.

[25] D. Cassioli, M. Z. Win, and A. F. Molisch, "The ultra-wide bandwidth indoor channel: from statistical model to simulations," *IEEE J. Sel. Areas Commun.*, vol. 20, no. 6, Aug. 2002.

[26] A. F. Molisch, D. Cassioli, C.-C. Chong, S. Emami, A. Fort, B. Kannan, J. Karedal, J. Kunisch, H. G. Schantz, K. Siwiak, and M. Z. Win, "A comprehensive standardized model for ultrawideband propagation channels," *IEEE Trans. Antennas Propag.*, vol. 54, pp. 3151–3166, Nov. 2006.

[27] K. Siwiak and A. Petroff, "A statistical model for indoor multipath propagation," *IEEE J. Sel. Areas Commun.*, vol. SAC-5, no. 2, pp. 128–137, Feb. 1987.

[28] B. Verbruggen, J. Craninckx, M. Kuijk, P. Wambacq, and G. Van der Plas, "A 2.2 mW 5b 1.75 GS/s folding flash ADC in 90 nm digital CMOS," in *Proc. ISSCC*, 2007.

[29] C. E. Shannon, "A mathematical theory of communication," *Bell Syst. Tech. J.*, vol. 27, pp. 379–423, 623–656, July-Oct. 1948.

[30] J. G. Proakis, *Digital Communications*, 4th edition. Addison-Wesley, 1972.

[31] E. Al-Hussaini and A. Al-Bassiouni, "Performance of MRC diversity systems for the detection of signals with Nakagami fading," *IEEE Trans. Commun.*, vol. 33, pp. 1315–1319, Dec. 1985.

[32] ——, "MRC performance for M-ary modulation in arbitrarily correlated Nakagami fading channels," *IEEE Trans. Commun.*, vol. 47, pp. 44–52, Jan. 1999.

[33] B. Sklar, *Digital Communications: Fundamentals and Applications*, 2nd edition. Prentice Hall PTR, 2001.

[34] A. Goldsmith, *Wireless Communications*, 1st edition. Cambridge University Press, 2005.

[35] A. Medi and W. Namgoong, "A high data-rate energy-efficient interference-tolerant fully integrated CMOS frequency channelized UWB transceiver for impulse radio," in *Proc. JSSC*, 2008.

[36] H. Kao, A. Chin, K. Chang, and S. McAlister, "A low-power current-reuse LNA for ultra-wideband wireless receivers from 3.1 to 10.6 GHz," in *Proc. SiRF07*, 2007.

[37] Y. Gao, K. Cai, Y. Zheng, and B.-L. Ooi, "A wideband CMOS multiplier for UWB application," in *Proc. ICUWB*, 2007.

[38] C. T. Fu and H. Luong, "A CMOS linear-in-dB high-linearity variable-gain amplifier for UWB receivers," in *Proc. ASSCC*, 2007.

[39] V. Lottici, A. D'Andrea, and U. Mengali, "Channel estimation for ultra-wideband communications," *IEEE J. Sel. Areas Commun.*, vol. 20, no. 9, pp. 1638–1645, Dec. 2002.


**Tianqi Wang** received the B.E. degree in 2004 in Communications Engineering, from Beijing University of Posts and Telecommunications, Beijing, China, and the M. Eng. degree in 2007 in Electrical and Computer Engineering, from Memorial University of Newfoundland, St. John's, Canada. He is currently working toward a Ph.D. degree at the Department of Electrical and Computer Engineering, University of Rochester, USA. His current research interests include wireless communications and cross-layer design in wireless sensor networks.

**Wendi B. Heinzelman** is an associate professor in the Department of Electricals and Computer Engineering at the University of Rochester, and she holds a secondary appointment as an associate professor in the Department of Computer Science. Dr. Heinzelman also currently serves as Dean of Graduate Studies for Arts, Sciences and Engineering at the University of Rochester. Dr. Heinzelman received a B.S. degree in Electrical Engineering from Cornell University in 1995 and M.S. and Ph.D. degrees in Electrical Engineering and Computer Science from MIT in 1997 and 2000, respectively. Her current research interests lie in the areas of wireless communications and networking, mobile computing, and multimedia communication.

Dr. Heinzelman received the NSF CAREER award in 2005 for her research on cross-layer architectures for wireless sensor networks, and she received the ONR Young Investigator Award in 2005 for her work on balancing resource utilization in wireless sensor networks. She is an Associate Editor for the IEEE TRANSACTIONS ON MOBILE COMPUTING, an Associate Editor for the *ACM Transactions on Sensor Networks* and an Associate Editor for *Elsevier Ad Hoc Networks Journal*. Dr. Heinzelman is a senior member of the IEEE and the ACM, and she is co-founder of the $N^2$ Women (Networking Networking Women) group.

**Alireza Seyedi** (S'95, M'04) received his B.S. degree from Sharif University of Technology, Tehran, Iran, in 1997 and his M.S. and Ph.D. degrees from Rensselaer Polytechnic Institute, Troy, NY, in 2000 and 2004, respectively, all in electrical engineering. Since 2007 he has been with the Faculty of the Electrical and Computer Engineering Department at the University of Rochester, where he currently is an Assistant Professor (Research). Prior to that, he was with Philips Research North America. His primary research interests are in the areas of Communications, Control, and their convergence. He is a Member of the IEEE Communications, Control and Signal Processing Societies.